Revista Brasileira de Ciências Ambientais
Brazilian Journal of Environmental Sciences

Sunflower seed husks as a cost-effective adsorbent for chloroquine removal from water

Cascas de semente de girassol como adsorvente econômico para a remoção de cloroquina de matriz aquosa

Isabela Arantes Ferreira[1], *Gessica Wernke*[1], *Alexandre Diório*[1], *Rosangela Bergamasco*[1], *Marcelo Vieira*[1]

ABSTRACT

The increased production and consumption of pharmaceuticals represent a potential environmental threat. Thus, advanced treatments are necessary to remove pharmaceutical products from water. A promising removal alternative is low-cost adsorbents, due to their availability, low processing, and favorable results. This study used sunflower seed husks (SSH) and chemically treated sunflower seed husks (TSSH) as bioadsorbents to remove chloroquine from water. Results showed that the pseudo-second-order is the kinetic model with the best fit for both adsorbents. As for isothermic models, the best fit for SSH was Langmuir, and for TSSH, Freundlich. Maximum adsorption capacities of q_e=168.09±22.98 mg/g and q_e=185.91±27.23 mg/g were found through the isothermic models for SSH and TSSH, respectively. In addition, SSH reached 80% of its initial adsorption capacity after three adsorption-desorption cycles, indicating physisorption and good applicability due to its reusability. Thus, SSH is an efficient adsorbent for chloroquine removal with excellent regeneration capacity, low production cost, and low waste production. This study serves as a model for the use of SSH in the removal of contaminants of emerging concern.

Keywords: agroindustrial residue; water pollution; bioadsorption; emerging contaminants; advanced water treatment.

RESUMO

O aumento da produção e consumo de produtos farmacêuticos representa uma ameaça potencial ao meio ambiente. Assim, são necessários tratamentos avançados para remover produtos farmacêuticos da água. Uma alternativa promissora de remoção são os adsorventes de baixo custo, devido à sua disponibilidade, baixo processamento e resultados favoráveis. Este estudo utilizou cascas de sementes de girassol (SSH) e cascas de sementes de girassol tratadas quimicamente (TSSH) como bioadsorventes para remover a cloroquina da água. Os resultados mostraram que a pseudo-segunda ordem é o modelo cinético com melhor ajuste para ambos os adsorventes. Quanto aos modelos isotérmicos, o melhor ajuste para SSH foi Langmuir, e para TSSH, Freundlich. Capacidades máximas de adsorção de qe=168,09±22,98 mg/g e qe=185,91±27,23 mg/g foram encontradas através dos modelos isotérmicos para SSH e TSSH, respectivamente. Além disso, o SSH atingiu 80% de sua capacidade inicial de adsorção após três ciclos de adsorção-dessorção, indicando fisissorção e boa aplicabilidade devido à sua reutilização. Assim, o SSH é um adsorvente eficiente para remoção de cloroquina com excelente capacidade de regeneração, baixo custo de produção e baixa produção de resíduos. Este estudo serve como modelo para o uso de SSH na remoção de contaminantes de preocupação emergente.

Palavras-chave: resíduos agroindustriais; poluição da água; bioadsorção; contaminantes emergentes; tratamento avançado de água.

[1]State University of Maringá – Maringá (PR), Brazil.
Correspondence author: Isabela Arantes Ferreira – State University of Maringá – Avenida Colombo, 5790, Bloco D90 – Zona 7 – CEP: 87020-900 – Maringá (PR), Brazil. E-mail: isarantes10@gmail.com

Conflicts of interest: the authors declare no conflicts of interest.
Funding: National Council for Scientific and Technological Development (CNPq), Process nº 133413/2021-0.
Received on: 01/07/2024. Accepted on: 06/10/2024.
https://doi.org/10.5327/Z2176-94781907

Introduction

Chloroquine diphosphate (CLQ) and its derivative hydroxychloroquine (HCLQ) are 4-aminoquinolone antibiotics, used in the treatment of malaria, autoimmune, and rheumatoid diseases (Plantone and Koudriavtseva, 2018; Zou et al., 2020). These drugs contain a nitrogen atom in their cyclic ring, increasing their solubility in water and promoting their incidence in aquatic environments, making them two of the most frequently detected pharmaceuticals in water and soil (Dabić et al., 2019).

The growth in production and consumption of pharmaceuticals poses a potential threat to the environment (Midassi et al., 2020). Studies have found that CLQ and HCLQ present chronic effects on zebrafish embryos and larvae (Silva et al., 2023) and cause alterations in enzymological and histopathological biomarkers in *Cyprinus carpio* (Ramesh et al., 2018). Moreover, CLQ may present synergistic ecotoxicological effects in a complex aquatic system. The combination of CLQ and copper ions, for example, results on higher toxicity for the reproduction of *Proales similis* than the drug alone (Rebolledo et al., 2022).

Environmental concentrations (μg L^{-1}) have been found for both CLQ and HCLQ. In Nigeria, Olaitan et al. (2014) detected CLQ in concentrations of 5 μg L^{-1} in groundwater and 0.11 μg L^{-1} in surface water. Nason et al. (2022) found concentrations of 50 μg L^{-1} for CLQ in the primary sludge of a wastewater treatment plant in the United States, demonstrating its intense consumption during the COVID-19 pandemic. In Italy, a concentration of 1.7 μg L^{-1} of HCLQ was detected in wastewater (Cappelli et al., 2022).

Thus, advanced treatment alternatives have been studied as potential pharmaceutical removal processes, such as photodegradation, electro-Fenton oxidation, membrane bioreactors, and adsorption processes, because conventional wastewater treatments do not completely remove pharmaceuticals from water (Sirés and Brillas, 2012; Delgado et al., 2019; Taoufik et al., 2020; Nippes et al., 2021).

The adsorption technique is a simple and economical alternative for contaminants removal from water (Mellah et al., 2018; Smiljanić et al., 2021). Low-cost adsorbents are made from naturally available materials and waste by-products, considered a sustainable alternative due to their environmental friendliness, energy efficiency, accessibility, recycling and reutilization approach, and cost reduction when compared to traditional adsorbents, such as activated carbon (Erto et al., 2013).

Sunflower seed husks (SSH) have been studied as a low-cost adsorbent for many contaminants. Literature shows the utilization of SSH in the removal of metal ions, like copper — Cu(II) (Stankovic et al., 2019) and nitrogen — Ni(II) (Tadayon et al., 2023); dyes, such as astrazon red (Kocadagistan and Kocadagistan, 2016), reactive blue 49, and reactive red 195 (Alhares et al., 2023); and contaminants of emerging concern, like the pesticides chlorfenvinphos, chlorpyrifos, simazine, and trifluralin (Rojas et al., 2015), and the drugs tetracycline, ciprofloxacin, ibuprofen, and sulfamethoxazole (Nguyen T.-B. et al., 2023; T.- Nguyen K.-T. et al., 2023).

Different biochars derived from low-cost adsorbents efficiently remove CLQ (Dada et al., 2021; Bankole et al., 2022; Santos et al., 2023). However, the aforementioned studies involved thermal treatment, which improves adsorbents characteristics and adsorption mechanisms but increases production costs. A study by Januário et al. (2023) investigated the adsorption of CLQ onto black soybean seed husks *in natura* with satisfactory removal rates but relatively low adsorption capacities when compared to biochar.

In this context, this paper aimed to study the adsorption of CLQ onto *in natura* SSH and chemically treated sunflower seed husks (TSSH) for the first time. We expected to provide a cost-effective alternative to biochar, with the chemical treatment improving adsorption capacities compared to the *in natura* adsorbent.

Materials and methodology

Contaminant

Chloroquine diphosphate ($C_{18}H_{26}ClN_3 \cdot 2H_3PO_4$, CAS number 50-63-5) was purchased from Galena Pharmaceuticals (Campinas, Brazil). CLQ has a molecular weight of 515.86 $g.mol^{-1}$, solubility of 50 $g.L^{-1}$ in water and pKa values of 8.38 and 10.18 (Sigma-Aldrich, 2024).

Preparation and treatment of the adsorbents

Sunflower (*Helianthus annuus*) seeds were purchased from a local store. The seeds were manually dehusked and the husks were washed with distilled water at 60°C (1:20 m/v ratio) until the washing water became clear. The *in natura* SSH were then separated, dried in an oven at 70°C for 24h, and finely grinded.

For TSSH, based on the chemical treatment proposed by Cusioli et al. (2021), the washed husks were mixed in a 0.1 M methanol solution (1:5 m/v ratio) for 4h at 500 rpm and room temperature (±25°C). After that, TSSH were washed with distilled water and mixed in a 0.1 M nitric acid solution (1:5 m/v ratio) for 1h at 500 rpm and room temperature. Then, TSSH were washed with distilled water again and dried in an oven at 70°C for 24h. After drying, they were finely grinded.

Adsorbent characterization

A FEI Quanta-250 scanning electron microscope was used to analyze the surface morphology of SSH and TSSH.

Physisorption of N_2 was conducted to determine the specific surface area, average pore diameter, total pore volume, mesopore volume and micropore volume. The adsorbents were previously submitted to degasification at 70°C for 6 h. During the experiment, the temperature of the samples was kept at -196.15°C (77K) in liquid hydrogen, and relative pressure (p/p_0) increased from 0.0016 to 0.9900 bar for adsorption and desorption. Results were analyzed using the Brunauer-Emmett-Teller (BET) equation.

Zeta potential experiments were conducted on a Delsa NanoC (Beckman Coulter) to determine the superficial charges of the adsorbents. The analysis was performed using five samples with 20 mL

of water and 0.02 g of adsorbent each. With 0.1 M sodium hydroxide (NaOH) and 0.1 M hydrogen chloride (HCl) solutions, the potential of hydrogen (pH) was corrected to points 2, 4, 6, 8, 10, and 12. The zeta potential at each point was then measured in triplicate.

Fourier transform infrared spectroscopy (FTIR) was used to determine functional groups of both adsorbents, before and after CLQ adsorption. The employed method was attenuated total reflectance (ATR) (VERTEX 70v, Bruker).

Adsorption experiments

Adsorbent concentration and pH effect

The adsorption of CLQ in both adsorbents was tested in batches and in duplicate, using a contaminant solution concentration fixed at 20 mg L^{-1}. Adsorbent mass (0.02–0.10 g), contaminant volume (0.02–0.10 L), and pH (5, 6, 7, 8, 9; and pH natural=5.71) were varied in the initial tests and the best-tested conditions were determined through adsorption capacity (q_e) and removal efficiency (RE). The solutions with SSH/TSSH samples were kept in sealed flasks in an orbital shaking incubator for 24h at 25°C, and 150 rpm. Then, the liquid phase was analyzed in a UV-Vis spectrometer (HACH DR 5000), at 343 nm wavelength, for equilibrium concentration (C_e) measurement. Then, with C_e measurements, q_e was calculated (Equation 1):

$$q_e = \frac{(C_i - C_e) \cdot V}{m} \quad (1)$$

Where:
q_e: adsorption capacity (mg g^{-1});
C_i and C_e: initial and equilibrium concentrations (mg L^{-1});
V: contaminant solution volume (L); and
m: adsorbent mass (g).

Adsorption kinetics

The adsorption kinetics study was performed in duplicate using 0.02 mg of adsorbent in 0.1 L of 20 mg L^{-1} contaminant solution, maintained in an orbital shaking incubator at 25°C and 150 rpm, at pH=6.0 (SSH) and 7.0 (TSSH). Final concentrations were analyzed at contact times varying from 2.5–1440 min. Adsorption capacities for each contact time were calculated through Equation 1.

Two kinetic models were applied to the experimental data in this study. The pseudo-first-order (PFO) model (Equation 2) was proposed by Lagergren (1898):

$$q_t = q_e[1 - e^{-k_1 t}] \quad (2)$$

Where:
q_t and q_e: adsorption capacities at time t and equilibrium (mg g^{-1});
t: contact time (min); and
k_1: pseudo-first-order adsorption rate constant (min^{-1}).

The pseudo-second-order (PSO) model (Equation 3) was proposed by Ho and McKay (1999):

$$q_t = \frac{k_2 q_e^2 t}{1 + k_2 q_e^t} \quad (3)$$

Where:
q_t and q_e: adsorption capacities at time t and equilibrium (mg g^{-1});
t: contact time (min); and
k_2: pseudo-second-order adsorption rate constant (g mg^{-1} min^{-1}).

The model adjustment and statistical analysis were conducted using the software Origin (OriginLab, 2018).

Adsorption isotherms

Adsorption equilibrium and temperature effect were studied in duplicate using three different temperatures: 25, 35, and 45°C. Contaminant concentration varied from 5 to 100 mg L^{-1} and studies were conducted using m=0.02 g, V=0.1 L, 150 rpm, t=24h, and pH=6.0 (SSH) and 7.0 (TSSH).

Langmuir and Freundlich isotherm models were applied utilizing Origin (OriginLab, 2018). The Langmuir model (Equation 4) assumed a defined number of active sites with no competition between them, and probability of adsorption at active sites as independent of adjacent sites (Langmuir, 1916):

$$q_e = \frac{q_m k_L C_e}{1 + k_L C_e} \quad (4)$$

Where:
k_L: Langmuir's isothermal constant (L mg^{-1}).

The Freundlich model (Equation 5), on the other hand, was applied to heterogeneous surfaces and assumed interactions between adsorbed molecules (Freundlich, 1906):

$$q_e = k_F C_e^{\frac{1}{n}} \quad (5)$$

Where:
k_F: Freundlich's isothermal constant [(mg L^{-1})(L g^{-1})$^{1/n}$].

The thermodynamic parameters were calculated using the isothermal results. Gibbs free energy (ΔG) was obtained through Equation 6.

$$\Delta G = -RTlnK_C \quad (6)$$

Where:
ΔG: Gibbs free energy;
K_C: adimensional equilibrium constant determined using experimental data.

To estimate enthalpy (ΔH) and entropy (ΔS) values, a graph of In (Kc) x 1/T was plotted. ΔH was obtained from the slope of the plotted line and ΔS, from the linear coefficient, as shown in Equation 7:

$$lnK_C = -\frac{\Delta H}{RT} + \frac{\Delta S}{R} \quad (7)$$

Where:
ΔH: enthalpy value; and
ΔS: entropy value.

Regeneration study

To investigate the reusability of SSH and TSSH, an adsorption experiment was conducted with 0.1 L of CLQ solution (20 mg L^{-1}) and 0.02 g of adsorbent, in duplicate. The loaded adsorbents were then filtered, dried at 70°C and stirred for 24h in 0.1 L of five different eluents: deionized water, pure methanol, pure ethanol, 0.1 M NaOH solution and 0.1 M HCl solution. The recycled SSH/TSSH were filtered, washed with deionized water and dried at 70°C. Three cycles of adsorption–desorption were conducted and desorption capacity (q_d) was calculated according to Equation 8.

$$q_d = \frac{C_d V}{m} \quad (8)$$

Where:
q_d: desorption capacity;
C_d: CLQ concentration after desorption (mg L^{-1});
V: solution volume (L); and
m: adsorbent mass (g).

Results and discussion

Adsorbent characterization

Scanning electron microscope (SEM) micrographs of SSH and TSSH (Figure 1) showed a heterogeneous and fibrous morphology, common to organic adsorbents, with high lignin and cellulose content (Januário et al., 2023).

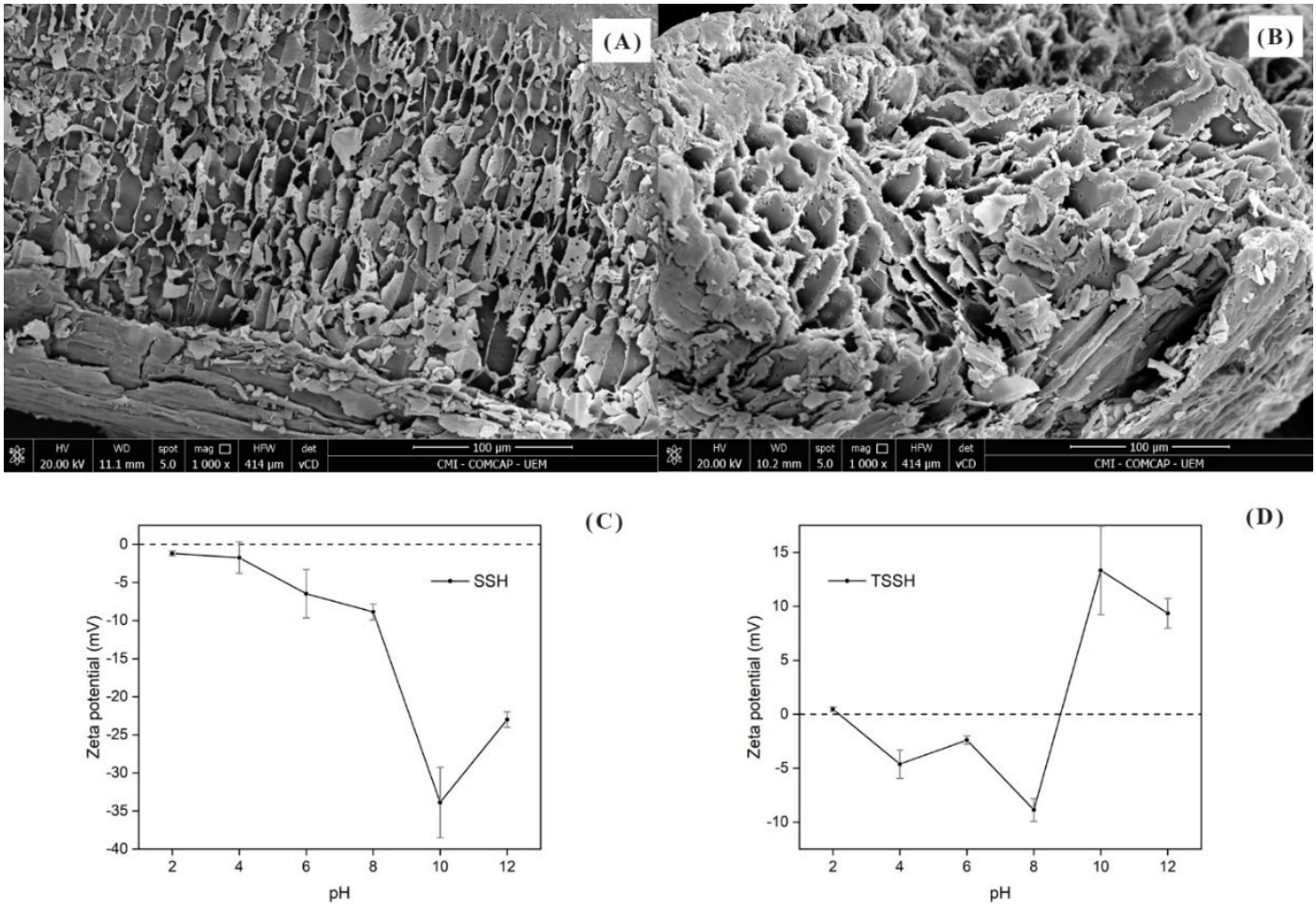

Figure 1 – (A) Micrograph of sunflower seed husks at 1000x; (B) Micrograph of treated sunflower seed husks at 1000x; (C) Zeta potential for sunflower seed husks; (D) Zeta potential for treated sunflower seed husks.

After chemical treatment, the pores became noticeably larger and more open, thus favoring the adsorption process. This could be due to oxidative lignin depolymerization by methanol (Sang et al., 2023) and nitric acid (Ahmad et al., 2021).

Zeta potential results for SSH and TSSH are displayed in Figure 1. For SSH, charges were negative for the entire examined pH range, suggesting possible exchangeable cations. Similar results were found for *in natura* SSH in the literature (Stankovic et al., 2019). As for TSSH, the material presented a different behavior, being negatively charged from approximately pH=2.0 to 9.0 and positively charged at very low and high pHs. Isoelectric points were approximately at pHs 2.0 and 8.8.

The physisorption of N_2 experiments results are displayed in Table 1. BET specific surface areas of 0.5257 m^2g^{-1} (SSH) and 0.8960 m^2g^{-1} (TSSH) were observed, which are similar to findings for other *in natura* bioadsorbents reported in the literature (Weber et al., 2013; Araujo et al., 2021; Tolić et al., 2021; Jaihan et al., 2022). Among the researched studies, only tangerine peel presented larger specific surface area than TSSH, with 0.965 m^2g^{-1} (Tolić et al., 2021). As for average pore diameter, the results were 71.43 Å (SSH) and 80.39 Å (TSSH); thus, both materials can be classified as mesoporous.

Total pore volume values were 0.000764 cm^3g^{-1} (SSH) and 0.001529 cm^3g^{-1} (TSSH). The chemical treatment increased total pore volume by 100%; micropore volume went from 0.000392 (SSH) to 0.000636 cm^3g^{-1} (TSSH), demonstrating that the chemical treatment successfully modified the adsorbent's surface. The researched studies suggest similar values to those found for the adsorbents; only *Guazuma ulmifolia* Lam. presented higher total pore volume than TSSH, with 0.00187 cm^3g^{-1} (Araujo et al., 2021).

Results for the FTIR-ATR analysis (Figure 2) showed organic functional groups, as is expected for lignocellulosic material (Vidovix et al., 2022). The peak at 3337 cm^{-1} suggests the presence of oxygen-hydrogen (O-H) bonds, related to oxygen groups (Januário et al., 2023). The peak intensity at 3337 cm^{-1} was higher for TSSH than SSH, indicating the changes caused by chemical treatment with methanol.

As for the peak at 2900 cm^{-1}, it indicates the presence of carbon-hydrogen (C-H) bonds, possibly H-bonds between CLQ and the adsorbents; weaker peaks at 1300–1400 cm^{-1}, associated with aromatic rings, indicate π-interactions (Vidovix et al., 2022). These are both possible adsorption mechanisms, especially H-bonds, presenting accentuated changes in detected intensity before and after adsorption. Aromatic rings were also more accentuated in TSSH than in SSH, possibly due to chemical modification.

The peak at 1732 cm^{-1} was more intense in TSSH, showing the presence of C=O bonds from esters. After CLQ adsorption, the peak shifted to 1598 cm^{-1}, indicating possible N-H interactions (Pradhan and Sandle, 1999; Cusioli et al., 2021). At 1225 cm^{-1}, the peak was caused by C-O stretches, present in glucose-cellulose bonds (Januário et al., 2023). The accentuated peak at 1025 cm^{-1} also indicates the presence of C-O and C-OH bonds, characteristics of lignin and celluloses (Cusioli et al., 2021), and the change in intensity from SSH to TSSH may also be an indicator of chemical modification.

The FTIR-ATR findings are comparable to those of the studies that used *in natura* SSH, in which peaks were detected at similar wavelengths (Tadayon et al., 2023). The results also indicate that the chemical treatment promotes changes in the superficial functional groups.

Table 1 – Results for physisorption of N_2.

Parameter	SSH	TSSH
BET specific surface area [m^2g^{-1}]	0.5257	0.8960
Total pore volume [cm^3g^{-1}]	0.000764	0.001529
Micropore volume [cm^3g^{-1}]	0.000392	0.000636
Average pore diameter [Å]	71.43	80.39

BET: Brunauer-Emmett-Teller equation; SSH: sunflower seed husks; TSSH: treated sunflower seed husks.

Adsorption experiments

Adsorbent concentration and pH effect

The conducted experiments achieved higher q_e for both SSH and TSSH when m=0.02 g and V=0.1 L, resulting in an adsorbent concentration of 200 mg L^{-1}. For SSH, q_e was highest at pH=6.0 (q_e=47.88 mg g^{-1}, RE=49.84%) and for TSSH at pH=7.0 (q_e=54.33 mg g^{-1}, RE=56.32%) (Figure 3). Those conditions were then used to perform the subsequent experiments.

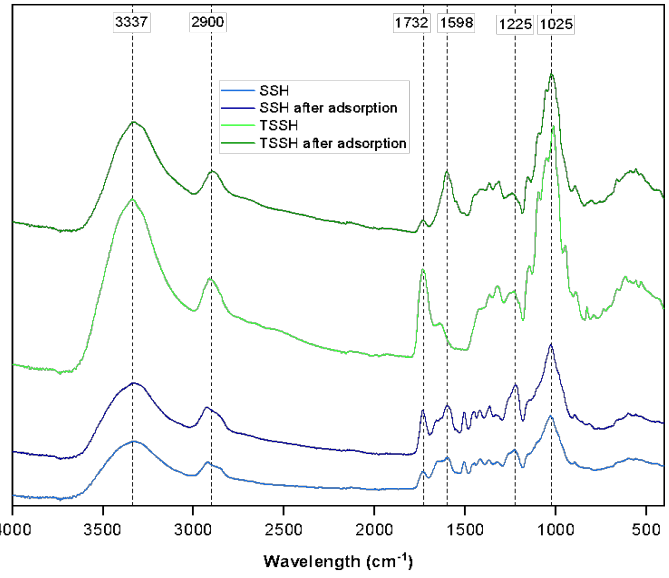

Figure 2 – Fourier transform infrared spectroscopy-attenuated total reflectance spectra for sunflower seed husks and treated sunflower seed husks, before and after adsorption.
FTIR: fourier transform infrared spectroscopy; ATR: attenuated total reflectance; SSH: sunflower seed husks; TSSH: treated sunflower seed husks.

The sharp decrease in adsorption capacity at pH 8.0 and 9.0 suggests the adsorption process works best with CLQ in its molecular form. When pH>8.38, CLQ is mostly in its ionizable form with negative charges in the solution due to its pKa value. As seen in the zeta potential study (Topic 2.1), both SSH and TSSH presented mostly negative surface charges in the 5.0–9.0 pH range, occurring electrostatic repulsion to the solution and thus decreasing adsorption capacity.

Adsorption kinetics

The kinetic experimental data obtained for SSH and TSSH are shown in Figure 4.

The curve for SSH presented a rapid increase in q_e in the initial minutes, with the removal rate of CLQ decreasing over time until stabilization at t=120 min, indicating that adsorption sites are readily available (Januário et al., 2023). The kinetic model that presented a better fit to the SSH experimental data was PSO, as seen in Table 2. After stabilization, the maximum value of q_e=47.31, standard deviation±1,07 mg/g, and RE=42.05% for SSH was obtained through the PSO kinetic model.

As for TSSH, similar behavior is observed, although the initial increase in q_e is less accentuated, and stabilization occurs only after t=720 min. The PSO kinetic model was also the best fit to the experimental data.

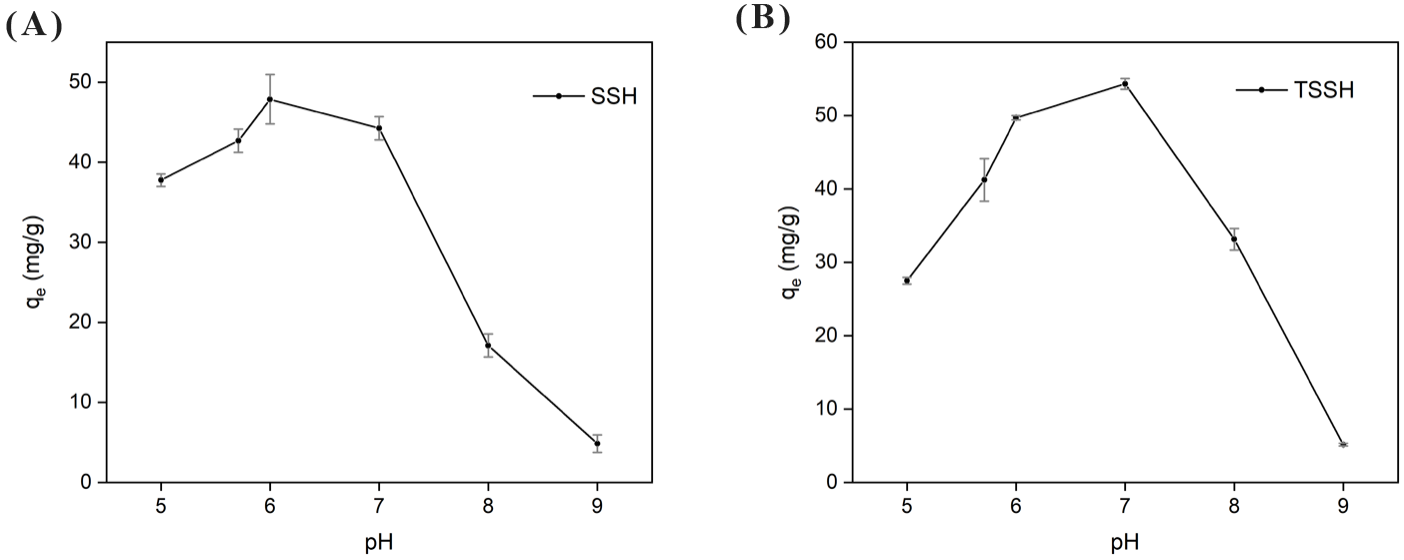

Figure 3 – Adsorption capacity at varying pHs for sunflower seed husks (A) and treated sunflower seed husks (B).
SSH: sunflower seed husks; TSSH: treated sunflower seed husks; q_e: adsorption capacity at equilibrium; pH: potential of hydrogen.

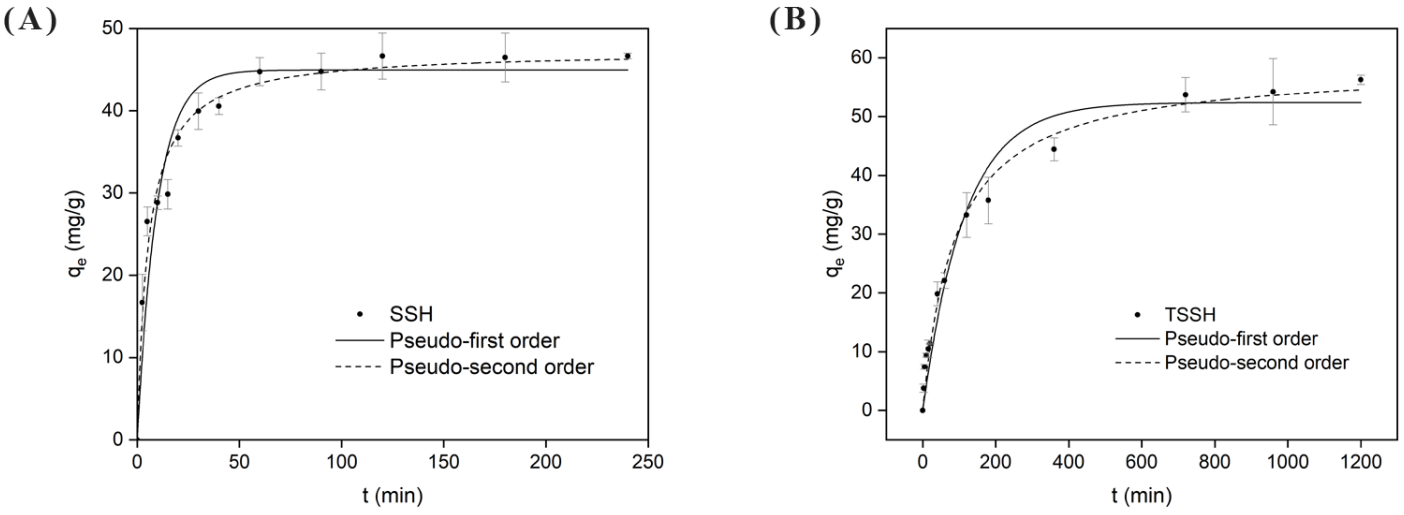

Figure 4 – Kinetics experimental data and model adjustment for sunflower seed husks and treated sunflower seed husks.
SSH: sunflower seed husks; TSSH: treated sunflower seed husks; q_e: adsorption capacity at equilibrium; t (min): time in minutes.

Parameter values obtained through the PSO model are displayed in Table 3, with a maximum value of q_e=57.88±2.99 mg/g and RE=57,08% for TSSH.

Other studies with CLQ also reported that the best fit for the adsorption kinetics was PSO, suggesting that the active sites of SSH and TSSH surfaces are directly related to the adsorption capacity (Dada et al., 2021).

Table 2 – Kinetic model parameters for sunflower seed husks and treated sunflower seed husks.

Kinetic model	Estimated parameter values	Experimental data SSH	Experimental data TSSH
PFO	q_{eq} (mg g^{-1})	44.95±0.05	52.40±2.12
	k_1 (min^{-1})	0.0102±0.0011	0.0087±0.0012
	R^2	0.9372	0.9637
	X^2	2.221	15.925
PSO	q_{eq} (mg g^{-1})	47.31±1.07	58.62±2.18
	k_2 (g mg^{-1} min^{-1})	0.00388±0.00006	0.00019±0.00003
	R^2	0.9782	0.9868
	X^2	4.645	5.789

SSH: sunflower seed husks; TSSH: treated sunflower seed husks; PFO: pseudo-first-order; PSO: pseudo-second-order; q_{eq}: adsorption capacity at equilibrium; k_1: pseudo-first-order adsorption rate constant; k_2: pseudo-second-order adsorption rate constant; R^2: coefficient of determination; χ^2: qui-square value.

Adsorption isotherms

The adsorption isotherms for SSH and TSSH are shown, respectively, in Figures 5A and 5B. Parameters for each isotherm model for both adsorbents are summarized in Table 3. Non-linear isothermal models were used.

It is observed that, for SSH at 25°C, the model that best fit the obtained experimental data was the Freundlich model, with a determination coefficient (R^2) of 0.97085 and reduced chi-square value (χ^2) of 27.212. For 35°C and 45°C, however, the best fit was the Langmuir model, with R^2=0.99504 and χ^2= 3.3326 for 35°C and R^2=0.97941 and χ^2=32.11738 for 45°C. This indicates that CLQ adsorption probably occurs in a monolayer and without interaction between adsorbate molecules for SSH (Vidovix et al., 2022).

For TSSH, the model that best fit the obtained experimental data for all tested temperatures was the Freundlich model, suggesting that adsorption occurs with interactions between molecules, which may be due to chemical treatment. When T=25°C, R^2= 0.9678 and χ^2=22.866. For T=35°C, R^2=0.9559 and χ^2=37.582. Finally, for T=45°C, R^2=0.9591 and χ^2=56.977.

The highest RE achieved were 82.61% (C=5 mg/L, T=35°C) for TSSH and 93.40% (C=10 mg/L, T=45°C) for TSSH.

For both adsorbents, a significant increase in q_e is observed with the change of temperature to 45°C. However, even at 25 and 35°C, and the maximum q_e found in this study is still higher than other results in literature for CLQ adsorption (Dada et al., 2021; Araujo et al., 2023; Santos et al., 2023).

Table 3 – Isotherm model parameters for sunflower seed husks and treated sunflower seed husks.

Adsorbent	Isotherms	Parameters	Temperature		
SSH			**25°C**	**35°C**	**45°C**
	Langmuir	q_m (mg g^{-1})	121.04±7.40	123.11±7.67	168.09±22.98
		k_L (L mg^{-1})	0.0256±0.0035	0.0293±0.0044	0.0155±0.0039
		R^2	0.98756	0.99504	0.96770
		X^2	11.760	3.333	39.218
	Freundlich	k_F (mgL^{-1})(Lg^{-1})$^{1/n}$	8.536±1.986	10.643±0.605	6.989±0.921
		1/n	0.5162±0.0575	0.4804±0.0141	0.5892±0.0322
		R^2	0.9709	0.9828	0.9850
		X^2	27.212	16.238	14.768
TSSH			**25°C**	**35°C**	**45°C**
	Langmuir	q_m (mg g^{-1})	123.14±9.96	133.92±13.24	185.91±27.23
		k_L (L mg^{-1})	0.0356±0.0075	0.0334±0.0084	0.0215±0.0067
		R^2	0.9632	0.9504	0.9386
		X^2	38.323	60.715	112.887
	Freundlich	k_F (mgL^{-1})(Lg^{-1})$^{1/n}$	13.238±1.762	13.850±2.242	11.336±2.126
		1/n	0.44395±0.0333	0.4465±0.0407	0.5354±0.0462
		R^2	0.9678	0.9559	0.9591
		X^2	22.866	37.582	56.977

SSH: sunflower seed husks; TSSH: treated sunflower seed husks; q_m: maximum adsorption capacity; R^2: coefficient of determination; χ^2: qui-square value; k_F: Freundlich's isothermal constant; k_L: Langmuir's isothermal constant

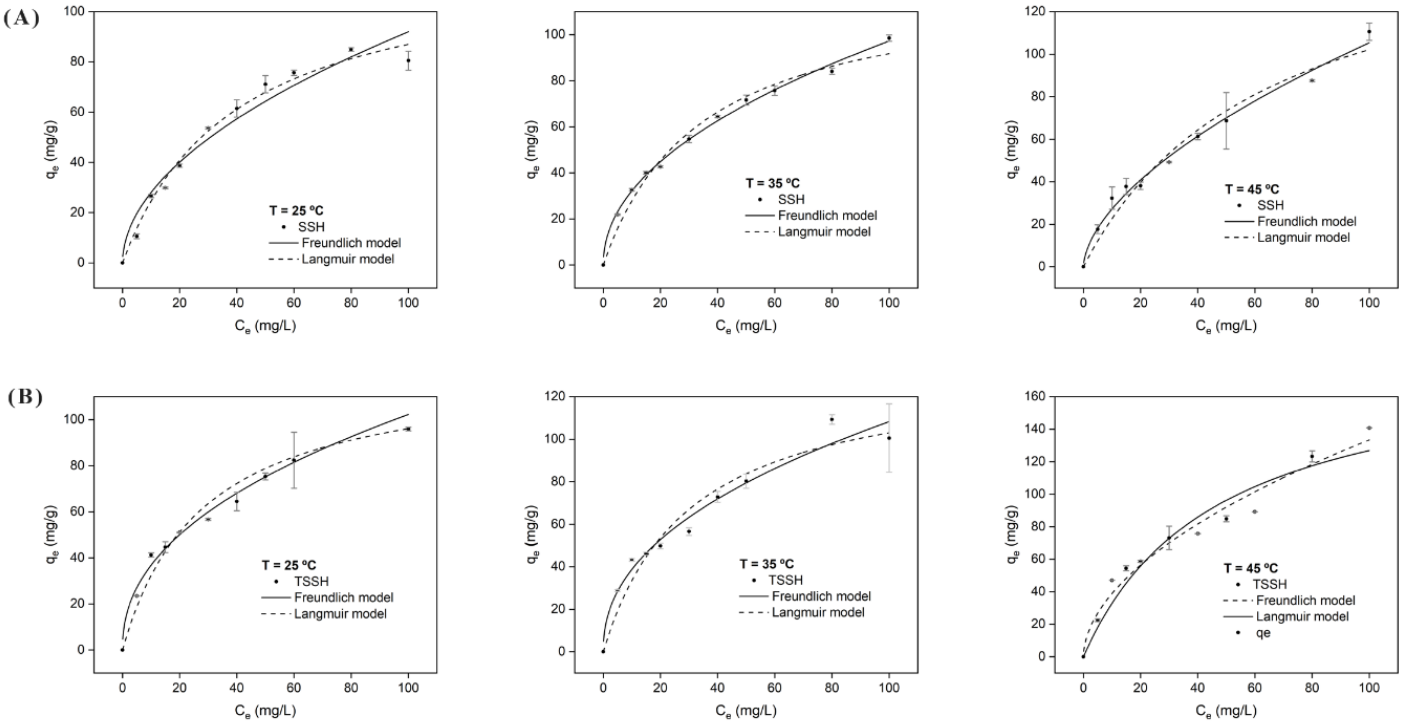

Figure 5 – Adsorption isotherms for sunflower seed husks (A) and treated sunflower seed husks (B).
SSH: sunflower seed husks; TSSH: treated sunflower seed husks; T: temperature; qe: adsorption capacity; Ce: equilibrium concentration.

For black soybean hulls *in natura*, a $q_e$max of 75.06 mg g^{-1} was obtained (Januário et al., 2023), which is approximately half of the maximum adsorption capacity found for SSH in this study. Soybean hulls residues functionalized with iron oxide nanoparticles reached $q_e$max=98.84 mg g^{-1} (Vidovix et al., 2022), while acid-activated hibiscus seed pods biochar achieved $q_e$max=161.29 mg g^{-1} (Bankole et al., 2022). Thus, the results indicate that SSH and TSSH present high adsorption capacity and are suitable for CLQ removal.

As for the thermodynamic parameters, Gibbs free energy (ΔG) values increased negatively for both SSH (from 0.628 at 25°C to -8.423 at 45°C) and TSSH (from -2.731 at 25°C to -3.628 at 45°C), which suggests a spontaneous process. The positive variation of enthalpy (ΔH=10.595 for SSH and ΔH=10.565 for TSSH) suggests an endothermic process, justifying the increase in adsorption capacity when T=45°C.

Enthalpy variation is also an indicator of the adsorption mechanism, since values between 2.10 and 20.90 kJ mol^{-1} suggest physisorption, while 80 to 200 kJ mol^{-1} indicate chemisorption (Cusioli et al., 2020). Thus, it is inferred that the adsorption of CLQ into SSH and TSSH occurs through physical mechanisms such as the H-bonds and π-interactions verified in the FTIR-ATR analysis (Figure 2).

Regeneration study

The eluent with the best desorption capacity was 0.1 M HCl solution. After three adsorption-desorption cycles, SSH was able to maintain over 80% of initial adsorption capacity (from 48.98 to 40.25 mg g^{-1}), indicating physisorption and good regenerative characteristics. For TSSH, however, adsorption capacity dropped to 55% over three cycles (from 58.73 to 32.47 mg g^{-1}), showing a decrease in regenerability and indicating partial chemisorption, consistent with FTIR-ATR results found in item 2.1.

Conclusion

Through this study, it was found that both SSH and TSSH are viable options for the removal of CLQ, presenting high maximum adsorption capacities and removal efficiencies at the lowest adsorbent concentration tested and neutral pH conditions, which is beneficial for full-scale applications.

For the SSH and TSSH, maximum adsorption capacities were reached at the adsorbent concentration of 200 mg/L, T=45°C, and pH=6.0 and 7.0, respectively. TSSH presented higher q_{emax} (185.91±27.23 mg g^{-1}) and RE (93.40%), but lower regeneration than SSH. Considering SSH reached a q_{emax}=168.09±22.98 mg g^{-1} and RE=82.61% under the same conditions, the increase of 10.60% in adsorption capacity and 10.79% in removal efficiency promoted by the studied chemical treatment does not justify the higher processing, costs, and production of pollution inherent to the modification process.

Thus, it is concluded that SSH is the most efficient biosorbent for CLQ, with outstanding regeneration capacity, low production costs, and

low waste generation. The developed methodology serves as a model for the use of SSH in the removal of other pharmaceutical compounds and contaminants of emerging concern, consisting of an environmentally friendly approach, with minimal waste and by-product production, low reagent consumption, low cost, and high reuse potential.

Acknowledgements

The authors thank the National Council for Scientific and Technological Development – CNPq for financial support and the Complex of Research Support Center – COMCAP/UEM for the characterization analysis.

Authors' contributions

FERREIRA, I.A.: conceptualization; methodology; writing – original draft. WERNKE, G.: writing – review & editing. DIÓRIO, A.: writing – review & editing. BERGAMASCO, R.: supervision. VIEIRA, M.: supervision.

References

Ahmad, Z.; Paleologou, M.; Xu, C.C., 2021. Oxidative depolymerization of lignin using nitric acid under ambient conditions. Industrial Crops and Products, v. 170, 113757. https://doi.org/10.1016/j.indcrop.2021.113757

Alhares, H.S.; Shaban, M.A.A.; Salman, M.S.; M-Ridha, M.J.; Mohammed, S.J.; Abed, K.M.; Ibrahim, M.A.; Al-Banaa, A.K.; Hasan, H.A., 2023. Sunflower husks coated with copper oxide nanoparticles for reactive blue 49 and reactive red 195 removals: adsorption mechanisms, thermodynamic, kinetic, and isotherm studies. *Water, Air, & Soil Pollution, v.* 234, (1), 35. https://doi.org/10.1007/s11270-022-06033-6

Araujo, L.A.; Bezerra, C.O.; Cusioli, L.F.; Rodríguez, M.T.; Gomes, R.G.; Bergamasco, R., 2021. Diclofenac adsorption using a low-cost adsorbent derived from *Guazuma ulmifolia* Lam. fruit via chemical and thermal treatment. Journal of Environmental Chemical Engineering, v. 9, (6), 106629. https://doi.org/10.1016/j.jece.2021.106629

Araujo, C.M.B.; Wernke, G.; Ghislandi, M.G.; Diório, A.; Vieira, M.F.; Bergamasco, R.; Sobrinho, M.A.M.; Rodrigues, A.E., 2023. Continuous removal of pharmaceutical drug chloroquine and safranin-o dye from water using agar-graphene oxide hydrogel: selective adsorption in batch and fixed-bed experiments. Environmental Research, v. 216, 114425. https://doi.org/10.1016/j.envres.2022.114425

Bankole, D.T.; Oluyori, A.P.; Inyinbor, A.A., 2022. Acid-activated *Hibiscus sabdariffa* seed pods biochar for the adsorption of chloroquine phosphate: prediction of adsorption efficiency via machine learning approach. South African Journal of Chemical Engineering, v. 42, 162-175. https://doi.org/10.1016/j.sajce.2022.08.012

Cappelli, F.; Longoni, O.; Rigato, J.; Rusconi, M.; Sala, A.; Fochi, I.; Palumbo, M.T.; Polesello, S.; Roscioli, C.; Salerno, F.; Stefani, F.; Bettinetti, R.; Valsecchi, S., 2022. Suspect screening of wastewaters to trace anti-COVID-19 drugs: potential adverse effects on aquatic environment. Science of The Total Environment, v. 824, 153756. https://doi.org/10.1016/j.scitotenv.2022.153756

Cusioli, L.F.; Quesada, H.B.; Andrade, M.B.; Gomes, R.G.; Bergamasco, R., 2021. Application of a novel low-cost adsorbent functioned with iron oxide nanoparticles for the removal of triclosan present in contaminated water. Microporous and Mesoporous Materials, v. 325, 111328. https://doi.org/10.1016/j.micromeso.2021.111328

Cusioli, L.F.; Quesada, H.B.; Baptista, A.T.A.; Gomes, R.G.; Bergamasco, R., 2020. Soybean hulls as a low-cost biosorbent for removal of methylene blue contaminant. Environmental Progress & Sustainable Energy, v. 39, (2), e13328. https://doi.org/10.1002/ep.13328

Dabić, D.; Babić, S.; Škorić, I., 2019. The role of photodegradation in the environmental fate of hydroxychloroquine. Chemosphere, v. 230, 268-277. https://doi.org/10.1016/j.chemosphere.2019.05.032

Dada, A.O.; Inyinbor, A.A.; Bello, O.S.; Tokula, B.E., 2021. Novel plantain peel activated carbon–supported zinc oxide nanocomposites (PPAC-ZnO-NC) for adsorption of chloroquine synthetic pharmaceutical used for COVID-19 treatment. Biomass Conversion and Biorefinery, v. 13, 9181-9193. https://doi.org/10.1007/s13399-021-01828-9

Delgado, N.; Capparelli, A.; Navarro, A.; Marino, D., 2019. Pharmaceutical emerging pollutants removal from water using powdered activated carbon: study of kinetics and adsorption equilibrium. Journal of Environmental Management, v. 236, 301-308. https://doi.org/10.1016/j.jenvman.2019.01.116

Erto, A.; Giraldo, L.; Lancia, A.; Moreno-Piraján, J.C., 2013. A Comparison between a low-cost sorbent and an activated carbon for the adsorption of heavy metals from water. Water, Air, & Soil Pollution, v. 224, (4), 1531. https://doi.org/10.1007/s11270-013-1531-3

Freundlich, H.M., 1906. Over the adsorption in solution. The Journal of Physical Chemistry A, v. 57, 385-470.

Ho, Y.S;. McKay, G., 1999. Pseudo-second order model for sorption processes. Process Biochemistry, v. 34, (5), 451-465. https://doi.org/10.1016/S0032-9592(98)00112-5

Jaihan, W.; Mohdee, V.; Sanongraj, S.; Pancharoen, U.; Nootong, K., 2022. Biosorption of lead (II) from aqueous solution using cellulose-based bio-adsorbents prepared from unripe papaya (*Carica papaya*) peel waste: removal efficiency, thermodynamics, kinetics and isotherm analysis. Arabian Journal of Chemistry, v. 15, (7), 103883. https://doi.org/10.1016/j.arabjc.2022.103883

Januário, E.F.D.; Vidovix, T.B.; Bissaro, C.A.; Defendi, R.O.; Jorge, L.M.M.; Bergamasco, R.; Vieira, A.M.S., 2023. Evaluation of the black soybean hulls agro-industrial waste for chloroquine removal from aqueous medium and treatment of multi-components. Journal of Dispersion Science and Technology, v. 45, (5), 1-11. https://doi.org/10.1080/01932691.2023.2186426

Kocadagistan, B.; Kocadagistan, E., 2016. The effects of sunflower seed shell modifying process on textile dye adsorption: kinetic, thermodynamic and equilibrium study. Desalination and Water Treatment, v. 57, (7), 3168-3178. https://doi.org/10.1080/19443994.2014.980329

Lagergren, S.Y. 1898. About the theory of so-called adsorption of solid substance. Kungliga Svenska Vetenskapsakademiens Handlingar, v. 4, 1-39.

Langmuir, I., 1916. The constitution and fundamental properties of solids and liquids. Part I. Solids. The Journal of Physical Chemistry A, v. 38, (11), 2221-2295. https://doi.org/10.1021/ja02268a002

Mellah, A.; Fernandes, S.P.S.; Rodríguez, R.; Otero, J.; Paz, J.; Cruces, J.; Medina, D.D.; Djamila, H.; Espiña, B.; Salonen, L.M., 2018. Adsorption of pharmaceutical pollutants from water using covalent organic frameworks. Chemistry European Journal, v. 24, (42), 10601-10605. https://doi.org/10.1002/chem.201801649

Midassi, S.; Bedoui, A.; Bensalah, N., 2020. Efficient degradation of chloroquine drug by electro-fenton oxidation: effects of operating conditions and degradation mechanism. Chemosphere, v. 260, 127558. https://doi.org/10.1016/j.chemosphere.2020.127558

Nason, S.L.; Lin, E.; Eitzer, B.; Koelmel, J.; Peccia, J., 2022. Changes in sewage sludge chemical signatures during a covid-19 community lockdown, part 1: traffic, drugs, mental health, and disinfectants. Environmental Toxicology and Chemistry, v. 41, (5), 1179-1192. https://doi.org/10.1002/etc.5217

Nguyen, T.-B.; Nguyen, T.-K.-T.; Chen, W.-H.; Chen, C.-W.; Bui, X.-T.; Patel, A.K.; Dong, C.-D., 2023. Hydrothermal and pyrolytic conversion of sunflower seed husk into novel porous biochar for efficient Adsorption of Tetracycline. Bioresource Technology, v. 373, 128711. https://doi.org/10.1016/j.biortech.2023.128711

Nguyen, T.-K.-T.; Nguyen, T.-B.; Chen, W.-H.; Chen, C.-W.; Patel, A.K.; Bui, X.-T.; Chen, L.; Singhania, R.R.; Dong, C.-D., 2023. Phosphoric acid-activated biochar derived from sunflower seed husk: selective antibiotic adsorption behavior and mechanism. Bioresource Technology, v. 371, 128593. https://doi.org/10.1016/j.biortech.2023.128593

Nippes, R.; Picoli, P.D.; Macruz, G.N.S.; Scaliante, M.H.N.O., 2021. A critical review on environmental presence of pharmaceutical drugs tested for the COVID-19 treatment. Process Safety and Environmental Protection, v. 152, 568-582. https://doi.org/10.1016/j.psep.2021.06.040

Olaitan, O.J.; Anyakora, C.; Bamiro, T.; Tella, A.T. 2014. Determination of pharmaceutical compounds in surface and underground water by solid phase extraction-liquid chromatography. Journal of Environmental Chemistry and Ecotoxicology, v. 6, (3), 20-26. https://doi.org/10.5897/JECE2013.0312

OriginLab, 2018. Origini(Pro). [Version 2018]. OriginLab Corporation, Northampton.

Plantone, D.; Koudriavtseva, T., 2018. Current and future use of chloroquine and hydroxychloroquine in infectious, immune, neoplastic, and neurological diseases: a mini-review. Clinical Drug Investigation, v. 38, (8), 653-671. https://doi.org/10.1007/s40261-018-0656-y

Pradhan, B.K.; Sandle, N.K., 1999. Effect of different oxidizing agent treatments on the surface properties of activated carbons. Carbon, v. 37, (8), 1323-1332. https://doi.org/10.1016/S0008-6223(98)00328-5

Ramesh, M.; Anitha, S.; Poopal, R.K.; Shobana, C., 2018. Evaluation of acute and sublethal effects of chloroquine (C18H26CIN3) on certain enzymological and histopathological biomarker responses of a freshwater fish. Cyprinus Carpio Toxicology Reports, v. 5, 18-27. https://doi.org/10.1016/j.toxrep.2017.11.006

Rebolledo, U.A.; Rico-Martínez, R.; Fernández, R.; Páez-Osuna, F., 2022. Synergistic effect of chloroquine and copper to the euryhaline rotifer *Proales similis*. *Ecotoxicology, v.* 31, (6), 1035-1043. https://doi.org/10.1007/s10646-022-02570-2

Rojas, R.; Morillo, J.; Usero, J.; Vanderlinden, E.; El Bakouri, H., 2015. Adsorption study of low-cost and locally available organic substances and a soil to remove pesticides from aqueous solutions. Journal of Hydrology, v. 520, 461-472. https://doi.org/10.1016/j.jhydrol.2014.10.046

Sang, Y.; Chen, H.; Khalifeh, M.; Li, Y., 2023. Catalysis and chemistry of lignin depolymerization in alcohol solvents - a review. *Catalysis Today*, v. 408, 168-181. https://doi.org/10.1016/j.cattod.2022.06.005

Santos, R.K.S.; Nascimento, B.F.; Araújo, C.M.B.; Cavalcanti, J.V.F.L.; Bruckmann, F.S.; Rhoden, C.R.B.; Dotto, G.L.; Oliveira, M.L.S.; Silva, L.F.O.; Sobrinho, M.A.M., 2023. Removal of chloroquine from the aqueous solution by adsorption onto açaí-based biochars: kinetics, thermodynamics, and phytotoxicity. Journal of Molecular Liquids, v. 383, 122162. https://doi.org/10.1016/j.molliq.2023.122162

Sigma-Aldrich, 2024. Safety data sheet for chloroquine diphosphate salt (Accessed July 22, 2024) at:. https://www.sigmaaldrich.com/BRi/en/sds/sigmalc6628?userType=undefined

Silva, I.F.; Enes, K.P.; Rocha, G.M.; Varotti, F.P.; Barbosa, L.A.; Thomé, R.G.; Santos, H.B., 2023. Toxicological effects of hydroxychloroquine sulfate and chloroquine diphosphate substances on the early-life stages of fish in the COVID-19 pandemic context. Journal of Environmental Science and Health, Part A, v. 58, (10), 825-830. https://doi.org/10.1080/10934529.2023.2238587

Sirés, I.; Brillas, E., 2012. Remediation of water pollution caused by pharmaceutical residues based on electrochemical separation and degradation technologies: a review. Environment International, v. 40, 212-229. https://doi.org/10.1016/j.envint.2011.07.012

Smiljanić, D.; Daković, A.; Obradović, M.; Ožegović, M.; Izzo, F.; Germinario, C.; de Gennaro, B., 2021. Application of surfactant modified natural zeolites for the removal of salicylic acid — a contaminant of emerging concern. Materials, v. 14, (24), 7728. https://doi.org/10.3390/ma14247728

Stankovic, S.; Sostaric, T.; Bugarcic, M.; Janicijevic, A.; Pantovic-Spajic, K.; Lopicic, Z., 2019. Adsorption of Cu(II) ions from synthetic solution by sunflower seed husks. Acta Periodica Technologica, v. 50, 268-277. https://doi.org/10.2298/APT1950268S

Tadayon, Y.; Bahrololoom, M.E.; Javadpour, S., 2023. An experimental study of sunflower seed husk and zeolite as adsorbents of Ni(II) ion from industrial wastewater. Water Resources and Industry, v. 30, 100214. https://doi.org/10.1016/j.wri.2023.100214

Taoufik, N.; Boumya, W.; Janani, F.Z.; Elhalil, A.; Mahjoubi, F.Z.; Barka, N., 2020. Removal of emerging pharmaceutical pollutants: a systematic mapping study review. Journal of Environmental Chemical Engineering, v. 8, (5), 104251. https://doi.org/10.1016/j.jece.2020.104251

Tolić, K.; Mutavdžić Pavlović, D.; Stankir, N.; Runje, M., 2021. Biosorbents from Tomato, Tangerine, and Maple Leaves for the Removal of Ciprofloxacin from Aqueous Media. Water, Air, & Soil Pollution, v. 232, (5), 218. https://doi.org/10.1007/s11270-021-05153-9

Vidovix, T.B.; Januário, E.F.D.; Bergamasco, R.; Vieira, A.M.S., 2022. Evaluation of agro-industrial residue functionalized with iron oxide magnetic nanoparticles for chloroquine removal from contaminated water. Materials Letters, v. 326, 132915. https://doi.org/10.1016/j.matlet.2022.132915

Weber, C.T.; Foletto, E.L.; Meili, L., 2013. Removal of tannery dye from aqueous solution using papaya seed as an efficient natural biosorbent. Water, Air, & Soil Pollution, v. 224, (2), 1427. https://doi.org/10.1007/s11270-012-1427-7

Zou, L.; Dai, L.; Zhang, X.; Zhang, Z.; Zhang, Z., 2020 hydroxychloroquine and chloroquine: A Potential and Controversial Treatment for COVID-19. Archives of Pharmacal Research, v. 43, (8), 765-772. https://doi.org/10.1007/s12272-020-01258-7